Argo-Two Decades: Global Oceanography, Revolutionized

Gregory C. Johnson, Shigeki Hosoda, Steven R. Jayne, Peter R. Oke, Stephen C. Riser, Dean Roemmich, Tohsio Suga, Virginie Thierry, Susan E. Wijffels, Jianping Xu

Annual Review of Marine Science

Argo—Two Decades: Global Oceanography, Revolutionized

Gregory C. Johnson,[1] Shigeki Hosoda,[2] Steven R. Jayne,[3] Peter R. Oke,[4] Stephen C. Riser,[5] Dean Roemmich,[6] Tohsio Suga,[7] Virginie Thierry,[8] Susan E. Wijffels,[3] and Jianping Xu[9]

[1]Pacific Marine Environmental Laboratory, National Oceanic and Atmospheric Administration, Seattle, Washington 98115, USA; email: gregory.c.johnson@noaa.gov

[2]Japan Agency for Marine-Earth Science and Technology, Kanagawa 237-0061, Japan; email: hosodas@jamstec.go.jp

[3]Department of Physical Oceanography, Woods Hole Oceanographic Institution, Woods Hole, Massachusetts 02543, USA; email: sjayne@whoi.edu, swijffels@whoi.edu

[4]Division of Marine and Atmospheric Research, Commonwealth Scientific and Industrial Research Organisation, Hobart, Tasmania 7001, Australia; email: peter.oke@csiro.au

[5]School of Oceanography, University of Washington, Seattle, Washington 98195, USA; email: riser@uw.edu

[6]Integrative Oceanography Division and Climate, Atmospheric Science, and Physical Oceanography Division, Scripps Institution of Oceanography, University of California, San Diego, La Jolla, California 92093, USA; email: droemmich@ucsd.edu

[7]Physical Oceanography Laboratory, Tohoku University, Sendai 980-8578, Japan; email: suga@tohoku.ac.jp

[8]Université de Brest, IFREMER, CNRS, IRD, Laboratoire d'Océanographie Physique et Spatiale, F-29280 Plouzané, France; email: vthierry@ifremer.fr

[9]Second Institute of Oceanography, Ministry of Natural Resources, Hangzhou 310012, China; email: sioxjp@139.com

Annu. Rev. Mar. Sci. 2022. 14:379–403

First published as a Review in Advance on June 8, 2021

The *Annual Review of Marine Science* is online at marine.annualreviews.org

https://doi.org/10.1146/annurev-marine-022521-102008

Keywords

anthropogenic climate change, ocean variability, ocean physics, weather prediction, ocean reanalysis

Abstract

Argo, an international, global observational array of nearly 4,000 autonomous robotic profiling floats, each measuring ocean temperature and salinity from 0 to 2,000 m on nominal 10-day cycles, has revolutionized physical oceanography. Argo started at the turn of the millennium,

growing out of advances in float technology over the previous several decades. After two decades, with well over 2 million profiles made publicly available in real time, Argo data have underpinned more than 4,000 scientific publications and improved countless nowcasts, forecasts, and projections. We review a small subset of those accomplishments, such as elucidating remarkable zonal jets spanning the deep tropical Pacific; increasing understanding of ocean eddies and the roles of mixing in shaping water masses and circulation; illuminating interannual to decadal ocean variability; quantifying, in concert with satellite data, contributions of ocean warming and ice melting to sea level rise; improving coupled numerical weather predictions; and underpinning decadal climate forecasts.

1. INTRODUCTION

Argo, an international scientific program begun in 1999, measures seawater properties and circulation of the subsurface ocean using autonomous profiling floats. It has been successful and influential, enabling more than 4,000 scientific publications since its inception, and the *New York Times* referred to Argo as "one of the scientific triumphs of the age" (Gillis 2014). Argo is motivated by the central roles of the ocean in Earth's climate. Oceans cover more than 70% of the planet's surface and contain more than 95% of its water. The land (which is relatively immovable) and the atmosphere (which has a relatively low heat capacity) also play important roles in Earth's climate, but the ocean's massive heat capacity, global circulation, and thermal inertia are key.

Accurate quantitative assessments of the ocean's roles in climate require continuous and global observations to define the ocean's state and reveal its full complexity. Prior to Argo, however, vast expanses of the world ocean, especially below the surface, were largely inaccessible. One of the earliest documented sets of useful ocean measurements was made around 1770. Benjamin Franklin analyzed observations of ocean temperature made on voyages between Europe and the English colonies to determine the structure and path of the Gulf Stream (Folger 1787). A hundred years later, the *Challenger* expedition (1872–1876) vastly increased the database by completing the first systematic survey of the world ocean, collecting ship-based measurements of temperature to depths as great as several thousand meters at more than 250 sites in the Atlantic, Pacific, and Indian Oceans [Tizard et al. 1965 (1885)].

Over the ensuing century, vessel and measurement technology continued to improve, and dedicated oceanographic laboratories with seagoing capabilities were founded. By the 1980s, oceanographers had gathered a nascent global data set consisting of a few thousand high-quality stations with full-depth temperature and salinity measurements, with a considerably smaller concomitant biogeochemical data set, and some early transient tracer observations. Analyses of these data illuminated a global, three-dimensional circulation composed of localized, deep sinking of water at high latitudes in the North Atlantic and around Antarctica, compensated by slow upwelling in the deep sea over the rest of the world ocean. This was all connected by deep flows away from the sinking regions and shallower return circulations. Such a global scenario had been hypothesized previously (Stommel 1957), and analyses of the data extant circa 1980 confirmed the idea (Warren 1981).

By the early 1980s, oceanographers had also realized that, despite increases in the global observational database and gains in our understanding of some aspects of the large-scale circulation, most of the subsurface ocean had still never been surveyed. The ambitious World Ocean Circulation Experiment (WOCE) was conceived to remedy this situation with a ship-based survey of the world ocean, covering all the main basins and sub-basins at several thousand sites. More than

4,000 new full-ocean-depth stations, sampling a wide range of physical and chemical parameters, were occupied as part of WOCE (King et al. 2001). Completing this survey took approximately a decade, and even now, more than 20 years later, the data in the WOCE archive constitute an incomparable reference data set, and their analysis continues.

An additional component of WOCE was the deployment of a newly developed instrument, the Autonomous Lagrangian Circulation Explorer (ALACE) (Davis et al. 1992). ALACE was a freely drifting float that spent most of its time at a depth of 1,000 m and ascended to the sea surface for a few hours to transmit its location via satellite at intervals of roughly 10 days, then descended back to 1,000 m for another 10 days. Its ascent and descent were controlled by the inflation and deflation of an external oil bladder. Differencing the positions between adjacent 10-day cycles yields estimates of the 10-day average velocity vector at 1,000 dbar. Hundreds of ALACE floats were deployed throughout the world ocean during WOCE. The resulting pioneering velocity data set (Davis 2005) provided the first-ever global view of the large-scale absolute velocity field in the deep sea. The beauty of ALACE was its simplicity: The floats were relatively inexpensive, no dedicated ship time was required for deployment or recovery, and the position data were available in near real time. The floats were capable of unattended operation for several years. Toward the end of WOCE, in the mid-1990s, a subset of ALACE floats were equipped with sensors to measure temperatures at selected pressures during each ascent, which were then transmitted by satellite along with float positions (Kwon & Riser 2004). By the end of the decade, some ALACE-type floats had been equipped with CTD (conductivity, temperature, and depth) instruments (Lavender et al. 2000).

While ship-based surveys over the past century were useful for exploring the subsurface ocean state, they were all onetime efforts with large gaps between ship tracks. By the late 1990s, climate change and the ocean's roles in it were becoming central issues. Providing answers and developing useful climate models required an examination of the time-dependent state of the global ocean. Repeating vessel-based WOCE-type sampling at the temporal and spatial scales required was not practical: Ships were expensive, and there were too few of them. However, making CTD measurements at hundreds or even thousands of locations in the world ocean at regular intervals from autonomous platforms seemed worth considering.

Informal musings on the possibilities of an array of ALACE-type instruments equipped with CTD instruments (which by then had become known as profiling floats) gave way to more formal discussions among groups of oceanographers, engineers, and program managers. In 1998, an implementation plan for what became known as Argo[1] emerged (Argo Sci. Team 1998). It called for a global array of roughly 3,000 CTD-equipped profiling floats profiling to 2,000 m at 10-day intervals, deployed at roughly 300-km intervals throughout the ice-free regions of the world ocean. It also stipulated that the data transmitted by the floats should be made freely available in real time over the rapidly developing internet.

The quantity of instrumentation, the global coverage, and the real-time, free availability of data were each forward-looking concepts; when considered together, the plan for Argo was revolutionary. The proposal was soon endorsed by the World Meteorological Organization as part of the Global Ocean Observing System. The first Argo float deployments took place in 1999, with the pace of deployments rapidly accelerating. An internet-based system to archive the data, make them available in real time, and provide a corrected version six months to a year later was created from scratch over the course of several years—a major milestone in itself that

[1]The name Argo invokes the synergies between the Jason satellite altimeter missions and the Argo program by recalling the legend of Jason and the Argonauts, who sailed the ship *Argo* in search of the Golden Fleece.

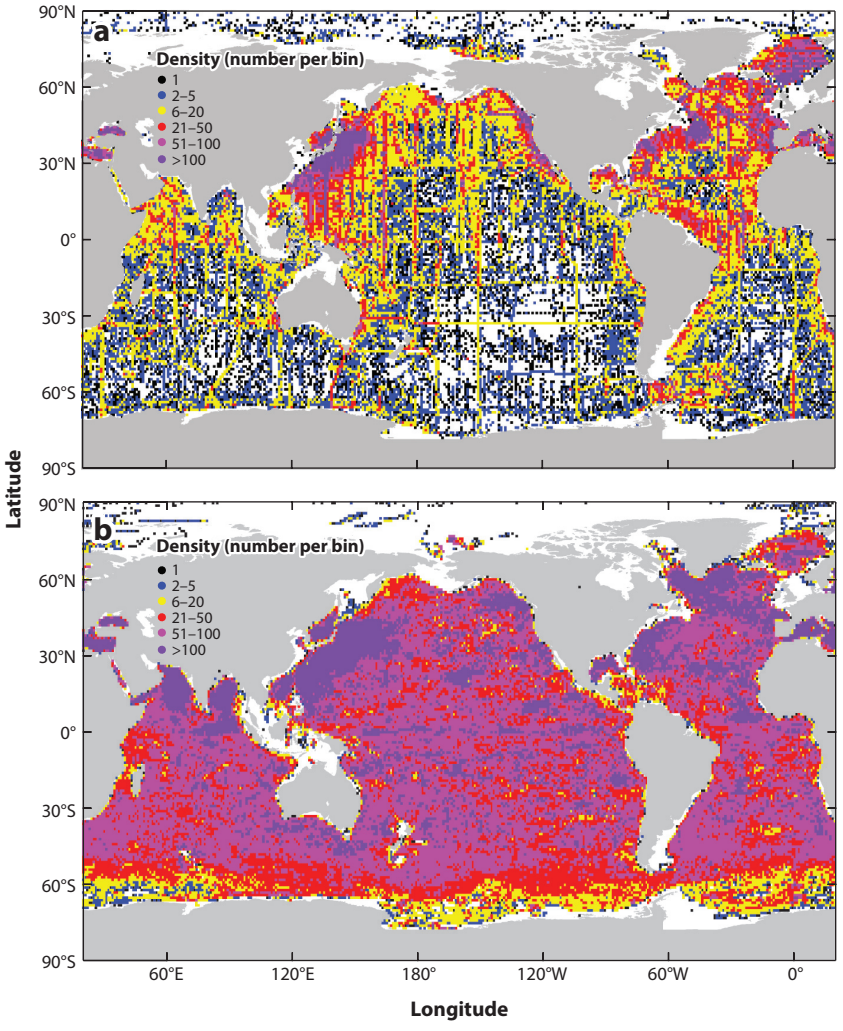

Figure 1

Spatial sampling density of subsurface ocean profiles of both temperature and salinity to a depth of 1,000 m or deeper in 1° latitude × 1° longitude bins, reported from (*a*) largely shipboard expeditions over the past 100 years [594,285 profiles from the World Ocean Database 2018 (Boyer et al. 2018)] and (*b*) Argo through mid-February 2021 (2,385,052 profiles from the Argo Global Data Assembly Centers). Figure updated from Riser et al. (2016).

still operates today (Wong et al. 2020). Around 2005, the Argo array first achieved sparse global coverage; by 2007, the array consisted of 3,000 floats; by 2012, more than 1 million profiles were available in the Argo global archive (Riser et al. 2016); by 2018, the 2 millionth profile had been collected; by 2020, the array was approaching 4,000 floats; and by the time of this writing, almost 2.4 million profiles had been reported, with some models profiling to full depth and others equipped with biogeochemical sensors. The quality and increasing quantity of Argo data over the past two decades have lived up to the revolutionary vision (**Figure 1**). Some examples of the advancements made possible by Argo follow.

2. ILLUMINATING THE DEPTHS WITH IMPROVED OCEAN CLIMATOLOGIES

For the first time, Argo has allowed the construction of contemporaneous observational global ocean climatologies of temperature, salinity, and velocity from the sea surface to 2,000 m, including the mean and seasonal cycle. By contrast, most pre-Argo climatologies were blended from sparser data that were spatially and temporally heterogeneous and heavily biased toward particular regions, seasons, and years. Argo-era climatologies have shed substantial light on many previously obscure or undiscovered ocean features worldwide.

2.1. The Mean Circulation and Water Mass Properties

Owing to their spatially and temporally unbiased sampling and high-quality near-global coverage, Argo data alone allow realistic three-dimensional monthly climatologies of temperature and salinity in the modern (or Argo) era from 0 to 2,000 m through objective analysis on isobaric surfaces (e.g., Roemmich & Gilson 2009). More elaborate Argo-based products further refine the picture of the oceanic mean state—for example, by providing statistics and preserving the temporal and spatial sampling capability of Argo (e.g., Gaillard et al. 2016) or by mapping on isopycnal surfaces with consideration of fronts and bathymetry (e.g., Schmidtko et al. 2013). Existing global full-depth temperature and salinity climatologies have also been updated with Argo data (e.g., Gouretski 2019).

Innovative analyses of Argo data have improved our picture of the upper-ocean structure. For example, a new algorithm to detect vertical density stratification minima (pycnostads) and maxima (pycnoclines) applied to individual Argo profiles yielded global ocean climatologies of subtropical mode waters and the permanent pycnocline (Feucher et al. 2019). This work greatly refined the canonical schematic for the density and spatial distribution of the subtropical mode waters (Hanawa & Talley 2001) and elucidated their relation to a remarkable double-center structure of the permanent pycnocline in the North Atlantic and both hemispheres of the Pacific.

Argo-based climatologies also encouraged novel approaches to distill the mean global ocean thermohaline structure. For example, by applying multivariate functional principal component analysis to a modern climatology (Schmidtko et al. 2013), Pauthenet et al. (2019) decomposed the thermohaline structures in the top 2 km of the global ocean into vertical thermohaline modes, with the first three modes capturing more than 92% of the observed temperature–salinity variance.

Displacements of Argo floats at their 1,000-dbar nominal parking pressure (e.g., Ollitrault & Rannou 2013) allowed the construction of global ocean 1,000-dbar velocity climatologies (e.g., Ollitrault & Colin de Verdière 2014). Climatologies of ocean steric height relative to 2,000 dbar based on Argo data readily depict major geostrophic flow features, including subtropical and subpolar gyre interiors with varying depth penetrations (e.g., Roemmich & Gilson 2009). The combination of the Argo-based mean circulation near 1,000 dbar and steric height climatologies delineated detailed relationships among the upper geostrophic circulation, mode waters, and the permanent pycnocline (Feucher et al. 2019), highlighting the deeper, thicker, and less stratified mode waters and permanent pycnocline in the North Atlantic, the basin where a strong overturning circulation is present.

The 1,000-dbar absolute velocity field is crucial to capture the mean geostrophic flow below the permanent pycnocline. Argo data reveal striking subthermocline zonal jets of alternating sign with short meridional scales and long zonal coherence in the tropical Pacific—signatures of two apparently distinct systems of altering westward and eastward jets (Cravatte et al. 2017), and slightly less distinct, but similar features in the two other ocean basins (**Figure 2**). The 1,000-dbar Argo velocity field together with a full-depth temperature and salinity climatology was used to obtain

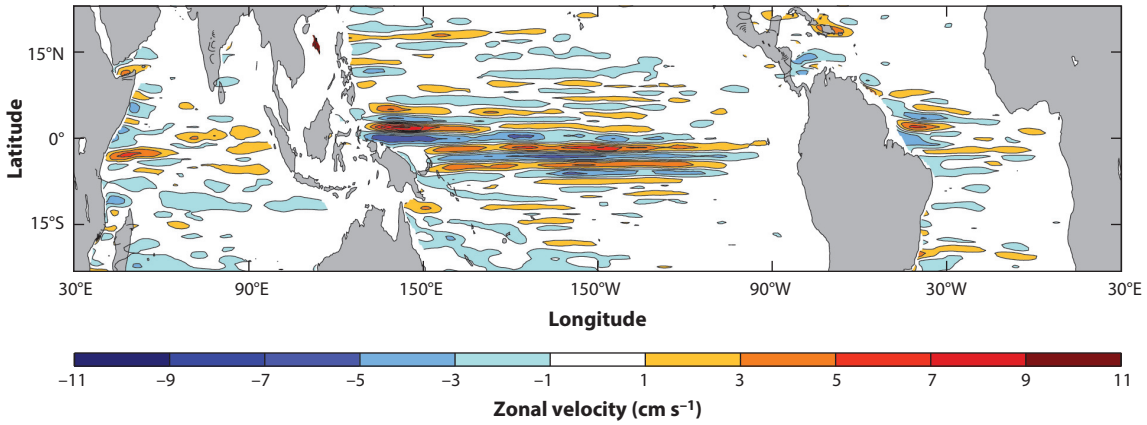

Figure 2

Mean zonal velocity at 1,000-dbar pressure estimated from 1,000-dbar Argo parking pressure displacements. Figure inspired by Zanowski et al. (2019) and expanded from the Pacific to the global tropics.

the full-depth mass transports of the global ocean. The analyses revealed that interior transports are roughly twice those derived from wind stress curl fields and suggest an important contribution of bottom torque (Colin de Verdière & Ollitrault 2016).

2.2. Seasonal Cycles

Seasonal cycles of three-dimensional temperature and salinity fields delineated by an Argo monthly climatology are largely consistent with those of sea surface temperature (SST), air–sea fluxes, and sea surface height (Roemmich & Gilson 2009), as well as wind-driven circulation theory (Giglio et al. 2013). A seasonal mixed-layer climatology from Argo demonstrates that while temperature changes dominate the seasonal cycle of mixed-layer density in most regions, salinity changes are the principal control in the tropical warm pools, Arctic, and Antarctic (Johnson et al. 2012).

More than 12 years of Argo data along with more than 22 years of altimetry allowed a detailed description of the upper-ocean seasonal circulation patterns in the equatorial Pacific (Gasparin & Roemmich 2017), including the superposition of a downwelling eastward-propagating intraseasonal Kelvin wave on a downwelling westward-propagating seasonal Rossby wave. The dominance of an annual Rossby wave in both the isothermal displacement and velocity fields at 1,000 dbar was also demonstrated using Argo data (Zanowski et al. 2019).

2.3. The Surface Mixed Layer

The ocean's surface mixed layer is a highly temporally and spatially variable feature that contributes to the exchange of heat and fresh water between the atmosphere and the ocean, water mass formation, and numerous other physical, chemical, and biological processes. A monthly climatology of mixed-layer depth was constructed in the previously data-poor Southern Ocean by applying the standard density and temperature threshold method (de Boyer Montegut et al. 2004) to individual Argo profiles (Dong et al. 2008), thus illuminating mode water formation there. A similar methodology was applied to the global Argo data to provide a global monthly climatology of mixed-layer depth (Hosoda et al. 2010).

Holte & Talley (2009) developed an algorithm to find the mixed-layer depth of individual Argo profiles. A monthly global climatology of mixed-layer depth was calculated using both

this algorithm and the standard threshold method and demonstrated that the former generally had better accuracy (Holte et al. 2017). A mixed-layer climatology based on this algorithm has been merged with an isopycnally based subsurface climatology to provide a consistent three-dimensional climatology on regular pressure grids that better preserves near-surface structure, water mass properties, and pycnocline strength (Schmidtko et al. 2013).

3. INNOVATIVE INSIGHTS INTO OCEAN PHENOMENA FROM BASIN THROUGH FINE SCALES

This section reviews the global insights Argo has allowed into key ocean phenomena, including subduction of water from the mixed layer to the ocean interior, fronts, eddies, mixing, and diffusion.

3.1. Subduction

The surface mixed layer lies between the atmosphere and the oceanic pycnoclines below. It directly exchanges properties such as heat, fresh water, carbon dioxide, and oxygen with the atmosphere. Subduction is the main mechanism for the transfer of fluid from the mixed layer to the permanent pycnocline. Subduction is driven by Ekman pumping, by lateral induction when horizontal currents flow across a sloping mixed-layer base, and by mesoscale eddies. Understanding the controlling factors of subduction and where and how much subduction occurs is vital to understanding the roles of the ocean in Earth's climate system and its evolution.

Argo data have been used to further the understanding of subduction processes in all oceanic basins and have revealed new details about their spatiotemporal patterns. For instance, the ventilation of the 18°C water in the subtropical North Atlantic is driven by vertical pumping near the coast and by the horizontal and temporal structure of the mixed-layer depths elsewhere (Trossman et al. 2009). In the North Pacific subtropical gyre, the westernmost mode waters are not directly subducted in the permanent pycnocline; they are entrained in the mixed layer farther east the following winter and preconditioned in ways that lead to the subduction of the easternmost mode water (Oka et al. 2011). In the Southern Ocean, subduction is regionally variable, with bathymetrically constrained hot spots of large subduction (Sallee et al. 2010).

Argo's four-dimensional observations of temperature and salinity allow investigation of the subduction and propagation of density-compensated temperature–salinity anomalies (spiciness) in the pycnocline (Portela et al. 2020, Sasaki et al. 2010), which may play an important role in decadal climate variability. These observations also allow accurate estimates of the annual mean subduction rate with much more certainty than those deduced from sporadic hydrographic and tracer data or numerical models (Qu et al. 2016, Toyama et al. 2015).

3.2. Fronts

Oceanic fronts are often boundaries between two different water masses, characterized by large horizontal density gradients and associated with relatively narrow, deep-reaching current cores and large surface velocities. Those currents play crucial roles in Earth's climate by redistributing oceanic properties, such as heat, fresh water, and nutrients. For example, the Antarctic Circumpolar Current is the world's largest current and is composed of a set of well-separated fronts in which isopycnals rise southward from the abyss to the ocean surface. This window from the surface to the deep ocean, with its vast capacity to store and transport heat and carbon, is key to the Southern Ocean's influences on Earth's climate. The properties, positions, and variability of these fronts have been major research subjects over the Argo era (e.g., Giglio & Johnson

2016). Owing to Argo's unprecedented sampling, these fronts could be studied through the use of classical methods based on combinations of water mass and dynamic properties (Giglio & Johnson 2016) and more objective methods, such as unsupervised classification (Jones et al. 2019). With a better knowledge of the fronts' characteristics, it was then possible to investigate their impacts on the Southern Ocean dynamics, such as the impact of cross-frontal exchange on the downstream evolution of Subantarctic Mode Water properties (Holte et al. 2013) or the link between frontal positions and the sign of eddy-induced subduction (Sallee et al. 2010).

Many studies have built on the complementarity between Argo and other data sets to investigate the impact of fronts on ocean dynamics and biogeochemistry. Together, the Aquarius satellite and Argo data well resolve detailed features and interannual variations of the sea surface salinity front along the Pacific equator (Qu & Yu 2014), a feature that delineates the eastern edge of the tropical western Pacific fresh water pool, which is linked closely to the El Niño/Southern Oscillation (ENSO), with its shifts in ocean circulation and precipitation. In the Mediterranean Sea, biogeochemical data from Argo floats and gliders highlighted the relevance of fronts in triggering primary production at the level of the deep chlorophyll maximum (Olita et al. 2017).

3.3. Ocean Footprints of Tropical Cyclones

Tropical cyclones derive their energy from warm upper-ocean temperatures. Their strong winds also drive vertical ocean mixing, together leading to cooler SSTs in the storms' wakes. These cold wakes have been studied using targeted profiling floats in process studies (e.g., Mrvaljevic et al. 2013). Chance encounters between tropical cyclones and Argo floats also provide insight into the basin-wide and global impact of these cold storm wakes. Argo observations were used to study the interaction between the ocean and Cyclone Nargis in 2008 to understand its rapid intensification (Lin et al. 2009). While the SST signature of cold wakes in the North Pacific disappear in approximately 10 days, Argo shows that their subsurface signatures persist for longer than a month (Park et al. 2011). Furthermore, on average, within the radius of gale force winds for strong tropical cyclones, there is a mixed-layer heat loss of approximately 160 MJ m^{-2}. On the basis of Argo data, it is estimated that tropical cyclones account for a substantial amount (1.87 PW) of the net annual heat transfer from the ocean to the atmosphere on the global scale (Cheng et al. 2015).

3.4. Eddies

Oceanic mesoscale eddies with length scales of approximately 50–300 km are ubiquitous, coherent ocean structures. They impact all dynamical components of the oceans and are key contributors to oceanic transports of heat, fresh water, dissolved CO_2, and other water properties, thereby influencing global climate change and the distribution of natural marine resources.

Vertical profiles from Argo floats systematically combined with satellite altimetry observations have afforded three-dimensional eddy reconstructions used to investigate eddies' characteristics and vertical structure at regional (e.g., Chaigneau et al. 2011) and global (Zhang et al. 2013) scales and their impact on the thermohaline structure of the ocean. Those reconstructions have been subsequently used to estimate the proportion and pathways of the eddy-induced heat transport (Sun et al. 2019, Zhang et al. 2014), confirming that mesoscale eddies trapping and transporting water masses within their cores as they propagate can advect large amounts of mass, heat, and fresh water (Dong et al. 2014). Agulhas rings and their role in advecting large quantities of heat across the South Atlantic are a striking example (Laxenaire et al. 2019, 2020).

The global nature of the Argo array offers unique opportunities to investigate the impacts of eddies on various oceanic processes and characteristics, such as Southern Ocean ventilation (Sallee et al. 2010) and mixed-layer depths at a global scale (Gaube et al. 2019), or to produce maps of

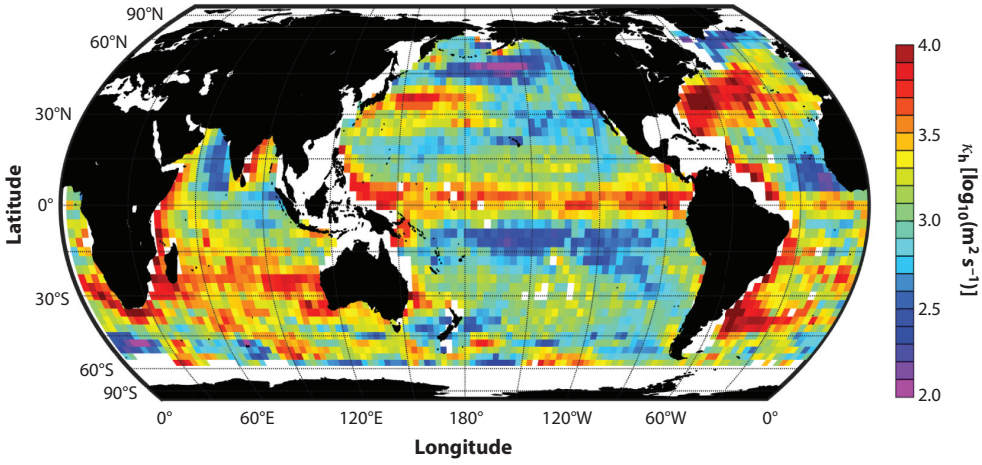

Figure 3

Horizontal eddy diffusivity derived from Argo float temperature and salinity profiles and Estimating the Circulation and Climate of the Ocean 2 (ECCO-2) eddy kinetic energy at 500-m depth (note logarithmic color scale). Figure courtesy of Sylvia Cole, inspired by Cole (2018) and Cole et al. (2015).

eddy-derived quantities, such as eddy available potential energy (Roullet et al. 2014) and eddy diffusivity at 1,000 m (Roach et al. 2018).

3.5. Mixing and Diffusion

The ocean is stirred and mixed by processes across a range of spatial scales. Observational investigations of stirring and horizontal eddy diffusivity in the upper ocean on the global scale would not be possible without Argo data (Cole 2018). The observed geographic distribution of horizontal eddy diffusivity varies by orders of magnitude (**Figure 3**), with the largest values in the strong current regions (Cole et al. 2015). Argo float trajectory data have been used to estimate Southern Ocean eddy diffusivity using a Lagrangian framework (Roach et al. 2016). This analysis, when expanded to the global ocean (Roach et al. 2018), is consistent to within a factor of two to three with results from Cole et al. (2015), indicating their robustness. Vertical mixing processes can also be quantified from Argo data: Global maps of turbulence from a parameterization of fine-scale mixing applied to Argo profile observations illuminate the rich spatial and temporal variability of mixing in the ocean (Whalen et al. 2015).

4. INTERANNUAL TO DECADAL VARIATIONS

Observation of interannual to decadal ocean variability is a key Argo objective (Argo Sci. Team 1998). Ocean and climate phenomena with substantial interannual to decadal variability include ENSO, meridional overturning circulations, gyre circulation changes (Roemmich et al. 2016), marine heat waves (MHWs) (Oliver et al. 2021), and water mass properties and formation rates. As discussed below, Argo data have been sufficient to average over mesoscale variability and extract large-spatial-scale interannual to decadal patterns and their temporal evolution since approximately 2004 over much of the global ocean.

4.1. El Niño/Southern Oscillation

ENSO is a major, global-scale climate phenomenon, driven by atmosphere–ocean interaction in the tropical Pacific and involving zonal displacement of very warm water across the tropical Pacific.

Changing oceanic conditions there covary with vertical convection in the troposphere driven by SST variability and exert global impacts through atmospheric teleconnections. The evolution of the tropical Pacific permanent thermocline is key to understanding ENSO, because it is related to the redistribution of ocean heat, salinity, and SST associated with this coupled ocean–atmosphere phenomenon.

Interannual variations of heat transport and warm water volume associated with ENSO have been quantitatively described using Argo data (Johnson & Birnbaum 2017, Roemmich & Gilson 2011) showing the vertical redistribution of global average ocean temperature during ENSO, with 0–100-m ocean warming and 100–500-m ocean cooling during El Niño and the opposite pattern holding during La Niña. Heat transport and redistribution associated with ENSO cause steric height variations. Argo aids understanding of the variability of sea surface height in terms of its steric and mass-related components (Piecuch & Quinn 2016). Interannual surface and subsurface salinity variability related to ENSO is also observed in Argo profiles (Nagano et al. 2017) related to sea surface height and advection (Gasparin & Roemmich 2016).

4.2. Atlantic Meridional Overturning Circulation

The Atlantic meridional overturning circulation (AMOC) consists of a net northward-flowing upper layer in the Atlantic, balanced by a net southward flow of deeper and denser waters. These opposing transports [on the order of 15 sverdrups (Sv)] vary with latitude and time. The northward meridional heat transport (on the order of 1 PW), which is closely related to this overturning cell, is climatically important because it moves heat from the tropics to higher latitudes in the Northern Hemisphere, moderating the climate of coastal Europe, among other things. Observations of the AMOC and meridional heat transport have been made at several latitudes, using several methodologies (Frajka-Williams et al. 2019).

In the Atlantic at 41°N, the flow is weak near the coasts, so broad-scale geostrophic transport from Argo with satellite altimetry gives an accurate representation of the basin-wide total northward limb of the AMOC, estimated as 17.6 Sv, with no apparent trend between 2002 and 2009 (Willis 2010). An update of this analysis reveals a decrease from 19 to 17 Sv in the five-year running mean transport relative to 1,000 dbar between 2008 and 2016. The combination of Argo and satellite altimetry was also used in estimates of the AMOC transport in the South Atlantic (Majumder et al. 2016), with results consistent with other methodologies.

Argo data are fundamental for closing the Atlantic heat budget. Air–sea flux estimates combined with Argo oceanic heat storage obtain the oceanic heat transport (Trenberth & Fasullo 2017) by integrating heat divergence southward from 90°N to any latitude of interest. The results were mostly consistent with estimates of meridional heat transport using other methods.

4.3. Ocean Circulation Changes

Variability in the large-scale wind forcing of the ocean causes spin-up or spin-down of the oceanic circulation, affecting mass, heat, and fresh water transport. Argo temperature and salinity profiles are used to calculate the relative geostrophic current in the upper layer of the global ocean. In addition, trajectory data obtained from float positions directly document current velocity at the drifting pressure of Argo floats, enabling estimation of absolute ocean velocity profiles.

Using Argo data, climatological meridional transports are estimated in each ocean basin for interior circulations and boundary currents. For example, net northward transport in the South Pacific is estimated as 20.6 ± 6.0 Sv across 32°S (Zilberman et al. 2014), with interannual variability proportional to the Southern Annular Mode. For all ocean basins, evaluation of the Sverdrup balance (Gray & Riser 2014) demonstrates consistency of wind stress and meridional geostrophic transport from Argo, especially in the tropics and subtropics.

The large volume of Argo data allows ocean velocities to be decomposed into average and eddy components (Katsumata 2016). Long-term changes associated with the acceleration of upper-ocean circulation are estimated using surface topographic data from satellites, along with Argo and WOCE hydrography (Giglio et al. 2012, Roemmich et al. 2016). With further accumulation of Argo profiles and trajectory data, gyre circulation variability and related heat and fresh water transport are described quantitatively.

4.4. Marine Heat Waves

Globally, long-term ocean warming is strongest at the surface, diminishing with depth (e.g., Wijffels et al. 2016). Therefore, the mean stratification of the surface layer increases as SST increases. Argo has helped resolve regional variability in SST warming that results in strong seasonal to interannual warm anomalies termed MHWs (Oliver et al. 2021). Large, persistent MHWs occurred in 2009–2010 in the central South Pacific, 2013–2016 and 2019–2020 in the northeast Pacific (Scannell et al. 2020) (**Figure 4**), and 2015–2019 in the Tasman Sea (Chiswell & Sutton 2020).

Strong and persistent MHWs have profound impacts on marine ecosystems that may lead to economic losses and other societal impacts. MHWs drive migratory responses and may cause decreased primary production, large-scale coral bleaching, toxic algal blooms, and declines in commercial fisheries. The addition of biogeochemical sensors to Argo floats for the Biogeochemical-Argo program will enable more comprehensive knowledge of ecosystem responses to MHWs. With Argo's global coverage, the relationship between increased stratification and decreased primary productivity can be more widely tested (e.g., Chiswell & Sutton 2020, Lozier et al. 2011).

Argo advances understanding of MHWs by revealing their subsurface structure and evolution (**Figure 4**). The Argo data set enables estimates of mixed-layer heat storage and advection terms that are important contributors (along with air–sea heat flux and mixing or entrainment) to the formation and duration of MHWs. MHW causality is complex, but anomalously weak air–sea heat loss and oceanic advection were factors in the 2013–2016 northeast Pacific episode (Bond et al. 2015), and salinity variability played a role in the 2019–2020 MHW there (Scannell et al. 2020). Argo's global coverage and expanding longevity will enhance the ability of ocean–atmosphere modeling to close the mixed-layer heat budget and predict MHW evolution.

4.5. Water Mass and Subduction Variability

Water masses, defined by their temperature–salinity characteristics, are formed by wind and buoyancy forcing at the sea surface. As newly formed waters are separated from the sea surface, specific water masses are identified as mode waters, intermediate waters, deep waters, and bottom waters, depending on their depth. Argo float data enable accurate documentation of water masses, including mode waters globally (Feucher et al. 2019), and investigation of the contributions of mode waters to the interannual variability of ocean heat content (Kolodziejczyk et al. 2019). The uniform and global Argo data set allows observation of the interannual variability of water masses in greater detail than was previously possible (Oka et al. 2015, Piron et al. 2017) and in locations where ship observations are challenging, such as the Southern Ocean (Giglio & Johnson 2016).

Anomalies in water mass properties and volume contain the ocean's memory of climate fluctuations, subducted subsurface and advected by ocean circulation. The processes, variability, and rate of subduction have been estimated in detail from Argo data (Qu et al. 2008, Toyama et al. 2015). Argo data were used to show an estimated weakening subduction rate associated with global warming of -3.44 ± 2.47 m y^{-2} (Wang et al. 2015). Variations in obduction (subduction's opposite) are also important for the reemergence of climate signals (Kawai et al. 2021).

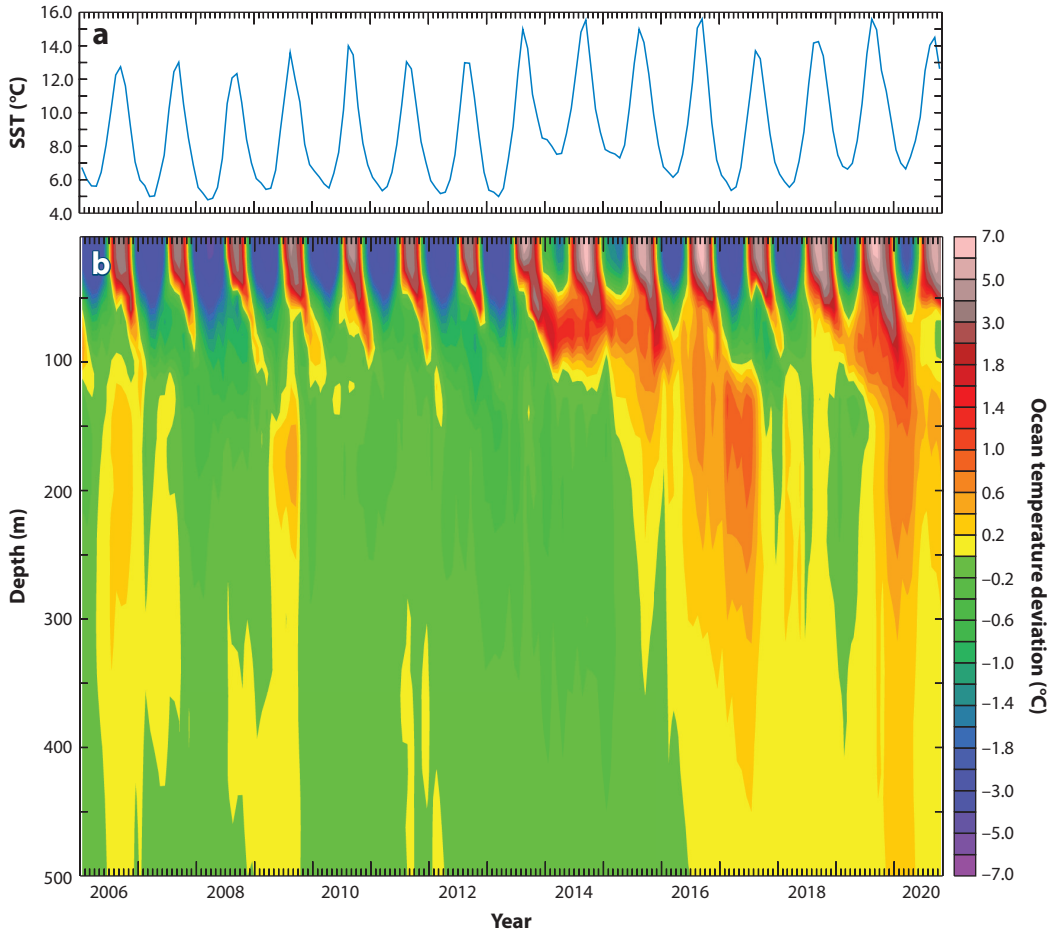

Figure 4

The northeast Pacific marine heat wave (here at 50°N, 145°W), from Argo data. (*a*) Sea surface temperature (SST). (*b*) Ocean temperature deviations from the 2006–2020 means from the surface to 500 m. The strong summer SST warming in 2013–2016 and 2019–2020 is mixed and/or subducted into subsurface layers.

5. GLOBAL CLIMATE INSIGHTS AND SYNERGIES WITH SATELLITES

Argo data, together with historical ocean and satellite data, provide valuable insights into long-term ocean trends that are central to understanding climate change and projecting future climates, including ocean warming, sea level rise, ocean salinity changes that reflect hydrological cycle changes, and increases in ocean stratification.

5.1. Earth's Energy Imbalance

Owing to the buildup of atmospheric greenhouse gases and the massive thermal inertia of the ocean, on the order of 1 W m^{-2} more energy enters the top of the atmosphere than exits it (Hartmann et al. 2014). This difference is often referred to as Earth's energy imbalance (EEI). Accurately measuring the small (<0.3%) difference of large spatially and temporally variable numbers at the top of the atmosphere is very difficult. Thus, most estimates of EEI have focused on

changes of heat energy storage in the climate system (von Schuckmann et al. 2020). For the ocean, which has absorbed approximately 90% of the EEI over the past few decades, this means estimating changes in global integrals of temperature anomalies.

Pioneering ocean warming estimates prior to Argo (Levitus et al. 2005) suffered from the effects of sparse spatial coverage and systematic instrumental measurement biases (Domingues et al. 2008). However, since 2005, more than 15 years of high-quality, year-round, near-global Argo ocean temperature data have greatly advanced estimates of ocean warming rates in the following ways. First, reliable seasonal cycles of temperature and salinity can be estimated locally throughout the globe using Argo (Roemmich & Gilson 2009). These estimates are vital for assessing anomalies in these variables from data taken in any time of year either during the Argo era or from as early as the *Challenger* expedition of the 1870s (Roemmich et al. 2012). Second, the Argo data's high quality has prompted investigations into instrumental biases (most notably those arising from variations in fall rates and temperature calibrations of expendable bathythermographs, which make up a substantial fraction of the global ocean temperature database from 1967 through the mid-2000s) (Abraham et al. 2013, Cheng et al. 2014, Gouretski & Reseghetti 2010). Third, sampling during Argo years increased so much that, coupled with the high quality of the data, it greatly reduced the uncertainty of earlier estimates of the EEI (mostly ocean warming), from 0.6 ± 0.4 W m^{-2} (2005–2010) to approximately 0.7 ± 0.1 W m^{-2} (2005–2015) (e.g., Johnson et al. 2016, Wijffels et al. 2016).

The warming trend detected by Argo is largest at the surface in the global average but can be seen all the way to the core array's 2,000-dbar profiling pressure (Johnson et al. 2019a). Regional pilot arrays of Deep Argo floats profiling to full water column depth are detecting warming trends below 2,000 dbar (Johnson et al. 2019b, 2020) that are most pronounced in the bottom waters spreading north from Antarctica and were quantified previously by ship-based repeat measurements (Purkey & Johnson 2013). Combined, these observations indicate that deep-ocean warming trends account for approximately 10% of the total EEI (Johnson et al. 2016, von Schuckmann et al. 2020). In addition, regional patterns of warming can be estimated using Argo and other data and related to climate variations (Johnson & Lyman 2020).

5.2. Sea Level Rise

Ocean warming contributes directly to sea level rise through the thermal expansion of seawater, accounting for approximately 40% of the globally integrated trend from 1993 through about 2016 (Cazenave et al. 2018). The other 60% comes from transfers of water (mostly melting ice) from the land to the ocean. While freshening from this melt also causes sea level rise by reducing seawater density, that contribution is much smaller than the other terms in the global average (Munk 2003). Strong synergies among Argo and data from two different sets of instruments on satellites allow quantification of the contributions. Satellite altimeters (from Jason and other missions) measure anomalies in sea level to great precision at all but the highest latitudes. Satellite gravimeters [Gravity Recovery and Climate Experiment (GRACE) and its follow-on] measure temporal variations in Earth's gravity field, from which ocean mass changes are estimated. Knowing the variations in sea level owing to thermal expansion from Argo, the changes in ocean mass from GRACE, and the changes in sea level from Jason and other altimeter missions allows the balancing of the sea level budget (Leuliette 2015), with excellent agreement down to monthly timescales (**Figure 5**).

5.3. Salinity and the Hydrological Cycle

Approximately 86% of evaporation and 78% of precipitation occur over the ocean, with most of the balance returning to the ocean as runoff from the land (Schanze et al. 2010). As the

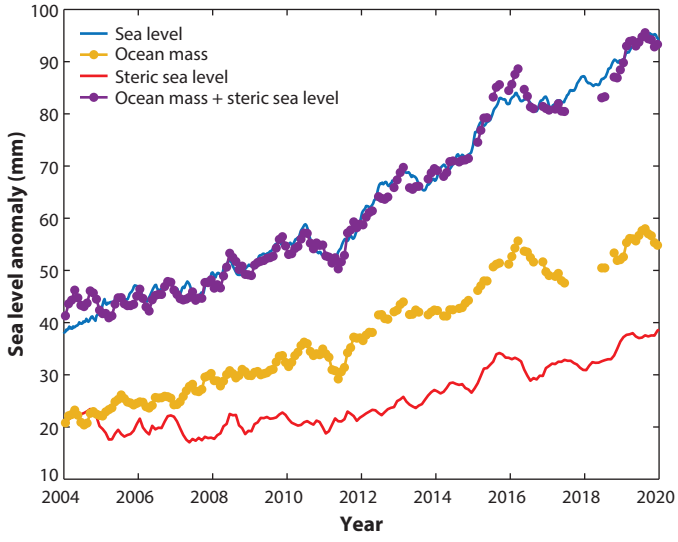

Figure 5

Monthly averaged global mean sea level anomaly (*blue line*), as observed by satellite altimeters from the NOAA Laboratory for Satellite Altimetry; monthly averaged global ocean mass (*yellow line with dots*), from the Gravity Recovery and Climate Experiment (GRACE) mission; monthly averaged global mean steric sea level (*red line*), from the Argo profiling float array; and monthly averaged global ocean mass plus monthly averaged global mean steric sea level (*purple line with dots*). All time series have been smoothed with a three-month filter. Figure adapted with permission from Thompson et al. (2020).

atmosphere warms, it can hold more water, which means more evaporation in some regions and more precipitation in others. Precipitation is extremely patchy and difficult to measure, especially over the ocean, where rain gauges can only be located on islands and buoys [although passive acoustic listening devices have been deployed on a few floats to measure rainfall (Yang et al. 2015), and more recently, satellite measurements (Hou et al. 2014) have provided global, but not continuous, estimates]. However, changes of ocean salinity can approximate a combination evaporation pan and rain gauge (Durack 2015). The net removal of fresh water by evaporation (or ice formation) and buildup from precipitation (or river runoff and ice melt) in the upper ocean over large spatial scales are reflected in salinity changes (absent changes in ocean mixing or advection). Again, Argo, by allowing the determination of a seasonal cycle in salinity around much of the globe, has improved the ability to analyze historical data and determine trends in upper-ocean salinity over decades.

Changes in surface salinity between historical (1960–1989) and Argo (2003–2007) data are consistent with an increase in evaporation in salty (e.g., subtropical) regions and an increase in precipitation in fresher (e.g., subpolar and tropical) ocean regions, as expected with a warming atmosphere (Hosoda et al. 2009). Changes in net values of precipitation minus evaporation over the ocean from 1970 to 2005 have been estimated from subsurface salinity changes at between −3% and +16%, depending on the region (Helm et al. 2010). Both subsurface and surface salinity trends estimated from 1950 to 2008 are also consistent with an increase in the hydrological cycle, including on basin scales, with the Atlantic becoming saltier and the Pacific fresher, and on more local scales, with the Bay of Bengal freshening as the Arabian Sea becomes saltier (Durack & Wijffels 2010).

5.4. Stratification Changes

Ocean warming and amplification of existing salinity patterns have generally been surface intensified. This pattern has led to an increase in stratification of several percent since 1960, with the bulk of that change owing to warming in the upper ocean, augmented at high latitudes and in the tropics by freshening and slightly offset in the subtropics by salinity increases (Li et al. 2020). Stratification increases have strong implications for climate, biogeochemistry, and ecosystems, including ocean warming and SST variability, as well as exchange of oxygen, nutrients, and carbon dioxide between the surface mixed layer and deeper ocean.

6. ARGO DATA IMPROVE OCEAN, WEATHER, AND CLIMATE MODELS

Argo data are routinely assimilated into ocean forecast, reanalysis, and seasonal prediction systems and are used to ground truth multiyear predictions and climate projections. Argo data are also increasingly used to initialize coupled numerical weather prediction (NWP) systems. Without Argo data, the quality of most ocean forecasts and reanalyses, and most seasonal predictions, would be substantially lower.

6.1. Ocean Forecasting and Reanalysis Systems

Ocean forecasting now underpins the operation of many marine industries (Bell et al. 2015). All credible ocean forecast systems (OFSs) assimilate Argo data, together with satellite data, to initialize the ocean state (e.g., Cummings et al. 2009). Initialized ocean models are integrated forward in time (typically for seven days), forced by surface fluxes from an NWP system. Ocean forecasts are widely used for safety at sea, efficiency, and conservation.

Many ocean reanalysis systems (ORAs) (Storto et al. 2019) have been developed in parallel with OFSs. They often use the same underlying model and the same data assimilation system. Some ORAs are eddy resolving (e.g., Artana et al. 2019), some are eddy permitting (e.g., Carton & Giese 2008), and some are coarse resolution (e.g., Balmaseda et al. 2013). All ORAs assimilate Argo data and depend on Argo data to constrain subsurface ocean properties (Storto et al. 2019).

Most OFSs and ORAs have been used to quantify the impact of Argo (and other) data on their forecasts or reanalyses (e.g., Fujii et al. 2019, Oke et al. 2009). When Argo data were withheld from the UK Meteorological Office's operational OFS for only one month, the global-averaged forecast errors for upper-ocean temperature and salinity increased by more than 5%, with the increased errors exceeding 2°C at 100-m depth for many parts of the ocean (Lea et al. 2015). When Argo data are withheld from the latest version of Ocean Reanalysis System 4 (ORAS4) (Zuo et al. 2019), a coarse-resolution ocean reanalysis shows that these types of reanalyses become unsuitable for realistically representing ocean variability (Fujii et al. 2019) (**Figure 6**). These results are typical of many OFSs and ORAs.

Most OFSs and ORAs have long been plagued by deep (>2,000 m) biases in temperature and salinity, largely as a consequence of scant deep measurements. A 1,200-float Deep Argo array (Johnson et al. 2015) promises to solve this problem. Constructing a synthetic database of Deep Argo measurements from one model and assimilating those synthetic observations into a different model showed that assimilation of data from Deep Argo floats may reduce the errors of temperature and salinity in the deep ocean (below 2,000-m depth) by as much as 50% (Gasparin et al. 2020).

6.2. Seasonal Prediction

Seasonal prediction systems typically employ coupled ocean–atmosphere models and, increasingly, coupled Earth system models (including sea-ice and land-surface models). They usually forecast

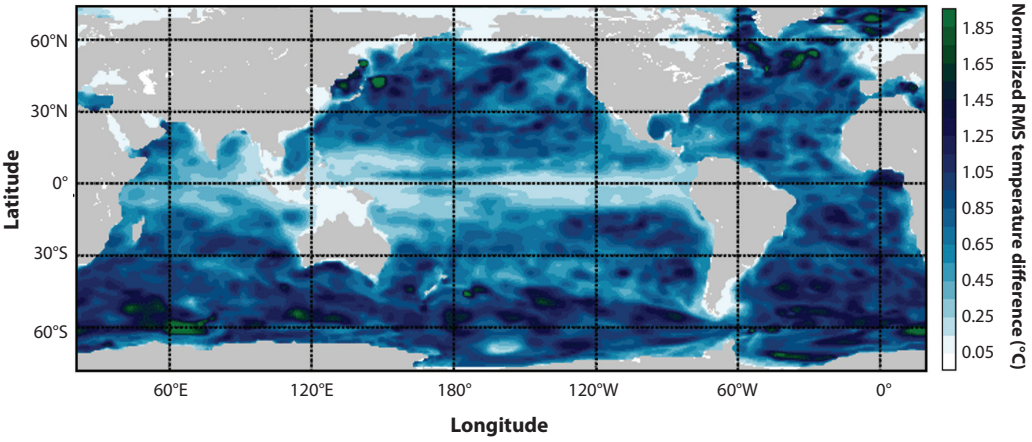

Figure 6

Normalized root-mean-square (RMS) difference in temperature for the upper 700 m from 2008 to 2014 between Ocean Reanalysis System 4 (ORAS4) with Argo data withheld and with Argo data assimilated. Fields are normalized against temporal standard deviations of temperature. Values exceeding unity indicate that errors in the reanalysis due to the neglect of Argo data are comparable to or exceed the signal amplitude. Figure adapted from Fujii et al. (2019) under a CC BY 4.0 license (**https://creativecommons.org/licenses/by/4.0**).

with lead times of three months to one year. Most of the skill of these systems stems from the ocean initialization and results from the longer timescales of variability (the memory) of the ocean (Balmaseda & Anderson 2009, Huang et al. 2021). Argo data are therefore the most critical ocean observations for initializing seasonal forecasts.

Many studies have assessed the impact of Argo data on seasonal prediction skill. Some studies have compared the skill of seasonal predictions for pre-Argo periods with those of contemporary periods, when the Argo data are nearly global, with mixed results (Huang et al. 2021, Kumar et al. 2015). Interpretation of results from these studies is problematic owing to differences in the predictability of the climate for these periods. For example, many relevant metrics were more predictable before 2000 (the pre-Argo period) than afterward (Zhao et al. 2016). Withholding Argo data and performing seasonal predictions for the same periods and events arguably provides better assessments, and all such studies find positive impacts. For example, assimilation of Argo data reduces forecast errors of temperature at three months of lead time by 0.2°C in the western equatorial Pacific, and increases the correlation skill of ENSO-related metrics by 0.1–0.2 at four months of lead time (Balmaseda et al. 2013). Inclusion of Argo data extends the forecast time for meaningful ENSO forecasts by 1.5 months (Stockdale et al. 2018). Many other similar studies also make clear that seasonal predictions benefit from Argo data, with increased skill at increased lead time.

6.3. Coupled Numerical Weather Prediction

Most NWP centers are moving toward coupled atmosphere–ocean models for short-range (approximately seven-day lead time) weather forecasting. As coupled systems are adopted, Argo data's importance and impact for NWP will certainly increase. However, despite the long-understood potential benefits of coupled prediction (Emanuel 1999), progress has been slow owing to significant scientific and technical challenges. Consequently, only a few studies (e.g., King et al. 2020) have explicitly assessed the impact of Argo data on coupled NWP.

In general, coupled NWP has shown greater positive impacts, compared with traditional atmosphere-only systems, for forecasts with longer lead times. For example, forecasts of the

Madden–Julian Oscillation have greater skill from a coupled system than from an uncoupled system for lead times of greater than 10 days (Woolnough et al. 2007). Coupled systems outperform atmosphere-only systems more at lower latitudes (Vellinga et al. 2020), with a more neutral benefit reported for coupled NWP at midlatitudes (Lea et al. 2015). Here, improved forecast skill can be ascribed largely to the ocean initialization using Argo data. For extreme events (e.g., Hurricane Sandy, in October 2012 in the North Atlantic), coupled prediction yields a better forecast of the timing and location of a hurricane's landfall than traditional NWP (King et al. 2020). This improvement is ascribed to the better representation of the Gulf Stream position in the coupled system, attributed largely to the impact of Argo data.

Widespread adoption of coupled NWP is progressing. The greatest challenge is consistent initialization of the atmosphere and ocean components of the coupled system, which is being tackled largely by coupled data assimilation (distinct from uncoupled assimilation). Coupled data assimilation—which allows oceanic observations, including Argo data, to directly influence analyses of the atmosphere and vice versa—is difficult but advancing (e.g., Fujii et al. 2021). The next generation of NWP systems will likely all rely on coupled ocean–atmosphere systems. For those systems, Argo data will be a foundational source of data for coupled initialization.

6.4. Decadal Prediction and Climate Projection

Much like coupled NWP, decadal prediction—increasingly referred to as near-term climate prediction (Kushnir et al. 2019)—has been hampered by difficulties in achieving consistent initialization of atmosphere and ocean models. Researchers have explored, with mixed results, coupled data assimilation (Fujii et al. 2021), parameter estimation (Zhang et al. 2020), multimodel ensemble prediction (Meehl et al. 2014), and more basic (Brune & Baehr 2020) but perhaps still useful approaches to initialization. Argo was quickly recognized as the most critical observation platform for initializing decadal predictions (Meehl et al. 2009). A modeling study, without data assimilation, demonstrated that decadal prediction of ocean heat content should be skillful (Yeager et al. 2012). Initializing the ocean with an Argo-based gridded product gave promising results (Robson et al. 2012), but model drift and coupled initialization remain as challenges. Ongoing efforts routinely rely on Argo data for initializations (Kushnir et al. 2019).

Climate projections do not assimilate observations (Eyring et al. 2016). But climate model outputs are routinely compared with Argo (and other) data to assess their representation of contemporary periods (e.g., Voldoire et al. 2019). This includes comparisons of mixed-layer depths (e.g., Roberts et al. 2020), upper-ocean heat content (e.g., Buckley et al. 2019), mean upper-ocean temperature and salinity (e.g., Robson et al. 2020), and even Argo-derived diffusivity (Zhu et al. 2020). Argo data clearly play an important role in the validation of systems used for climate projections, providing a comprehensive ground truth that guides model development and model tuning.

SUMMARY POINTS

1. The Argo array, which started with a few floats in 2000, now observes temperature and salinity in the upper half of the ocean volume (to 2,000 m) for its core mission, with almost 4,000 active floats distributed over most of the global ocean.
2. Now numbering almost 2.4 million, high-quality profiles from core Argo, reported in near real time, have underpinned more than 4,000 scientific papers and are routinely used to improve ocean, weather, and climate forecasts and nowcasts.

3. Ocean climatologies (of the long-term mean, seasonal cycle, or monthly values) using temperature, salinity, and velocity data have confirmed existing theories, allowed novel discoveries, and prompted new hypotheses regarding ocean circulation, water mass formation, and their drivers.
4. Analyses of Argo data have also illuminated diverse oceanic physical processes, including water mass formation, subduction, eddy influences on ocean circulation and water masses, frontal structure and dynamics, and even global patterns of mixing and diffusivity.
5. The Argo record, now approaching two decades in length, is increasingly allowing insightful analyses of interannual to decadal ocean variability, including the global redistributions of heat and salt with the El Niño/Southern Oscillation, variations in gyre and meridional overturning circulation strength, and the evolution of marine heat waves, to name a few.
6. Argo data, combined with historical in situ observations and contemporaneous satellite data, have illuminated key climate phenomena with greatly increased certainty, including Earth's energy imbalance, contributions of ocean warming versus land-ice melting to sea level rise, and increases in the hydrological cycle with atmospheric warming, as observed in the amplification of ocean salinity patterns.
7. Argo data have been key to advances in ocean reanalyses that combine various observations in a dynamical framework to fill gaps in observations and in ocean and weather nowcasts and forecasts, as well as validating the ability of climate models to represent contemporary ocean conditions.

FUTURE ISSUES

1. Core Argo, the mission measuring physical parameters from 0 to 2,000 m, will extend its capabilities through expansion into marginal seas and seasonally ice-covered regions in the climate-critical, rapidly warming high latitudes, as well as through increases in float numbers in the dynamic tropics and western boundary current extensions.
2. Deep Argo has begun regional pilot arrays, with the goal of having more than 1,200 floats reporting measurements from the sea surface to the seafloor to monitor deep-ocean warming and circulation changes.
3. Biogeochemical-Argo, which aims to add oxygen, nitrate, pH, fluorescence, optical backscatter, and downwelling irradiance sensors to 1,000 floats deployed around the globe, will greatly expand the contributions of Argo beyond the physical realm.
4. Synergies with new observing system elements will increase the usefulness of Argo data, including the new surface water and ocean topography altimeter for submesoscale oceanography and glider arrays for coastal and boundary current interactions with the open ocean.
5. Argo data will become increasingly vital for climate and weather forecasts as progress is made on the challenging task of initializing coupled models.
6. Continued improvements in sensor accuracy and stability, as well as float and sensor energy efficiency and longevity, will be crucial to maintaining and improving the Argo array.

DISCLOSURE STATEMENT

The authors are currently members (except for V.T., who has previously been a member) of the International Argo Steering Team (T.S. and S.E.W. are cochairs), and all receive funding from their various national agencies to work on the Argo program, either of which might be perceived as affecting the objectivity of this review.

ACKNOWLEDGMENTS

This article is Pacific Marine Environmental Laboratory contribution number 5210. G.C.J. is supported by NOAA Research. Argo data were collected and made freely available by the International Argo Project and the national programs that contribute to it. Argo is a pilot program of the Global Ocean Observing System.

LITERATURE CITED

Abraham JP, Baringer M, Bindoff NL, Boyer T, Cheng LJ, et al. 2013. A review of global ocean temperature observations: implications for ocean heat content estimates and climate change. *Rev. Geophys.* 51:450–83

Argo Sci. Team. 1998. *On the design and implementation of Argo: an initial plan for a global array of profiling floats*. Int. CLIVAR Proj. Off. Rep. 21, GODAE Rep. 5, GODAE Int. Proj. Off., Bur. Meteorol., Melbourne, Aust.

Artana C, Provost C, Lellouche J-M, Rio M-H, Ferrari R, Sennéchael N. 2019. The Malvinas Current at the confluence with the Brazil Current: inferences from 25 years of Mercator Ocean reanalysis. *J. Geophys. Res. Oceans* 124:7178–200

Balmaseda M, Anderson D. 2009. Impact of initialization strategies and observations on seasonal forecast skill. *Geophys. Res. Lett.* 36:L01701

Balmaseda M, Mogensen K, Weaver AT. 2013. Evaluation of the ECMWF ocean reanalysis system ORAS4. *Q. J. R. Meteorol. Soc.* 139:1132–61

Bell MJ, Schiller A, Le Traon P-Y, Smith NR, Dombrowsky E, Wilmer-Becker K. 2015. An introduction to GODAE OceanView. *J. Oper. Oceanogr.* 8(s1):s2–s11

Bond NA, Cronin MF, Freeland H, Mantua N. 2015. Causes and impacts of the 2014 warm anomaly in the NE Pacific. *Geophys. Res. Lett.* 42:3414–20

Boyer TP, Baranova OK, Coleman C, Garcia HE, Grodsky A, et al. 2018. *World Ocean Database 2018*. Tech. ed. AV Mishonov. NOAA Atlas NESDIS 87, Natl. Cent. Environ. Inf., Natl. Ocean. Atmos. Adm., Washington, DC. **https://www.ncei.noaa.gov/products/world-ocean-database**

Brune S, Baehr J. 2020. Preserving the coupled atmosphere-ocean feedback in initializations of decadal climate predictions. *WIREs Clim. Change* 11:e637

Buckley MW, DelSole T, Lozier MS, Li L. 2019. Predictability of North Atlantic sea surface temperature and upper-ocean heat content. *J. Clim.* 32:3005–23

Carton JA, Giese BS. 2008. A reanalysis of ocean climate using Simple Ocean Data Assimilation (SODA). *Mon. Weather Rev.* 136:2999–3017

Cazenave A, Meyssignac B, Ablain M, Balmaseda M, Bamber J, et al. 2018. Global sea-level budget 1993–present. *Earth Syst. Sci. Data* 10:1551–90

Chaigneau A, Le Texier M, Eldin G, Grados C, Pizarro O. 2011. Vertical structure of mesoscale eddies in the eastern South Pacific Ocean: a composite analysis from altimetry and Argo profiling floats. *J. Geophys. Res. Oceans* 116:C11025

Cheng L, Zhu J, Cowley R, Boyer T, Wijffels S. 2014. Time, probe type, and temperature variable bias corrections to historical expendable bathythermograph observations. *J. Atmos. Ocean. Technol.* 31:1793–825

Cheng L, Zhu J, Sriver RL. 2015. Global representation of tropical cyclone-induced short-term ocean thermal changes using Argo data. *Ocean Sci.* 11:719–41

Chiswell SM, Sutton PJH. 2020. Relationships between long-term ocean warming, marine heat waves and primary production in the New Zealand region. *N. Z. J. Mar. Freshw. Res.* 54:614–35

Cole ST. 2018. Investigating small-scale processes from an abundance of autonomous observations. In *ALPS II: Autonomous and Lagrangian Platforms and Sensors; A Report of the ALPS II Workshop Held February 21–24, 2017, La Jolla, California*, ed. D Rudnick, D Costa, K Johnson, C Lee, M-L Timmermans, pp. 25–27. **https://geo-prose.com/pdfs/ALPS-II.pdf**

Cole ST, Wortham C, Kunze E, Owens WB. 2015. Eddy stirring and horizontal diffusivity from Argo float observations: geographic and depth variability. *Geophys. Res. Lett.* 42:3989–97

Colin de Verdière A, Ollitrault M. 2016. A direct determination of the world ocean barotropic circulation. *J. Phys. Oceanogr.* 46:255–73

Cravatte S, Kestenare E, Marin F, Dutrieux P, Firing E. 2017. Subthermocline and intermediate zonal currents in the tropical Pacific Ocean: paths and vertical structure. *J. Phys. Oceanogr.* 47:2305–24

Cummings J, Bertino L, Brasseur P, Fukumori I, Kamachi M, et al. 2009. Ocean data assimilation systems for GODAE. *Oceanography* 22(3):96–109

Davis RE. 2005. Intermediate-depth circulation of the Indian and South Pacific Oceans measured by autonomous floats. *J. Phys. Oceanogr.* 35:683–707

Davis RE, Webb DC, Regier LA, Dufour J. 1992. The Autonomous Lagrangian Circulation Explorer (ALACE). *J. Atmos. Ocean. Technol.* 9:264–85

de Boyer Montegut C, Madec G, Fischer AS, Lazar A, Iudicone D. 2004. Mixed layer depth over the global ocean: an examination of profile data and a profile-based climatology. *J. Geophys. Res.* 109:C12003

Domingues CM, Church JA, White NJ, Gleckler PJ, Wijffels SE, et al. 2008. Improved estimates of upper-ocean warming and multi-decadal sea-level rise. *Nature* 453:1090–93

Dong C, McWilliams JC, Liu Y, Chen D. 2014. Global heat and salt transports by eddy movement. *Nat. Commun.* 5:3294

Dong S, Sprintall J, Gille ST, Talley L. 2008. Southern Ocean mixed-layer depth from Argo float profiles. *J. Geophys. Res. Oceans* 113:C06013

Durack PJ. 2015. Ocean salinity and the global water cycle. *Oceanography* 28(1):20–31

Durack PJ, Wijffels SE. 2010. Fifty-year trends in global ocean salinities and their relationship to broad-scale warming. *J. Clim.* 23:4342–62

Emanuel KA. 1999. Thermodynamic control of hurricane intensity. *Nature* 401:665–69

Eyring V, Bony S, Meehl GA, Senior CA, Stevens B, et al. 2016. Overview of the Coupled Model Intercomparison Project Phase 6 (CMIP6) experimental design and organization. *Geosci. Model Dev.* 9:1937–58

Feucher C, Maze G, Mercier H. 2019. Subtropical mode water and permanent pycnocline properties in the World Ocean. *J. Geophys. Res. Oceans* 124:1139–54

Folger T. 1787. Chart of the Gulf Stream. In *Philosophical and Miscellaneous Papers*, ed. B Franklin, facing p. 122. London: C. Dilly

Frajka-Williams E, Ansorge IJ, Baehr J, Bryden HL, Chidichimo MP, et al. 2019. Atlantic Meridional Overturning Circulation: observed transport and variability. *Front. Mar. Sci.* 6:260

Fujii Y, Ishibashi T, Yasuda T, Takaya Y, Kobayashi C, Ishikawa I. 2021. Improvements in tropical precipitation and sea surface air temperature fields in a coupled atmosphere–ocean data assimilation system. *Q. J. R. Meteorol. Soc.* 147:1317–43

Fujii Y, Rémy E, Zuo H, Oke P, Halliwell G, et al. 2019. Observing system evaluation based on ocean data assimilation and prediction systems: on-going challenges and a future vision for designing and supporting ocean observational networks. *Front. Mar. Sci.* 6:417

Gaillard F, Reynaud T, Thierry V, Kolodziejczyk N, von Schuckmann K. 2016. In situ–based reanalysis of the global ocean temperature and salinity with ISAS: variability of the heat content and steric height. *J. Clim.* 29:1305–23

Gasparin F, Hamon M, Rémy E, Traon P-YL. 2020. How Deep Argo will improve the deep ocean in an ocean reanalysis. *J. Clim.* 33:77–94

Gasparin F, Roemmich D. 2016. The strong freshwater anomaly during the onset of the 2015/2016 El Niño. *Geophys. Res. Lett.* 43:6452–60

Gasparin F, Roemmich D. 2017. The seasonal march of the equatorial Pacific upper-ocean and its El Niño variability. *Prog. Oceanogr.* 156:1–16

Gaube P, McGillicuddy DJ Jr., Moulin AJ. 2019. Mesoscale eddies modulate mixed layer depth globally. *Geophys. Res. Lett.* 46:1505–12

Giglio D, Johnson GC. 2016. Subantarctic and polar fronts of the Antarctic Circumpolar Current and Southern Ocean heat and freshwater content variability: a view from Argo. *J. Phys. Oceanogr.* 46:749–68
Giglio D, Roemmich D, Cornuelle B. 2013. Understanding the annual cycle in global steric height. *Geophys. Res. Lett.* 40:4349–54
Giglio D, Roemmich D, Gille ST. 2012. Wind-driven variability of the subtropical North Pacific Ocean. *J. Phys. Oceanogr.* 42:2089–100
Gillis J. 2014. In the ocean, clues to change. *New York Times*, Aug. 12. **https://www.nytimes.com/2014/08/12/science/in-the-ocean-clues-to-change.html**
Gouretski V. 2019. A new global ocean hydrographic climatology. *Atmos. Ocean. Sci. Lett.* 12:226–29
Gouretski V, Reseghetti F. 2010. On depth and temperature biases in bathythermograph data: development of a new correction scheme based on analysis of a global ocean database. *Deep-Sea Res. I* 57:812–33
Gray AR, Riser SC. 2014. A global analysis of Sverdrup balance using absolute geostrophic velocities from Argo. *J. Phys. Oceanogr.* 44:1213–29
Hanawa K, Talley LD. 2001. Mode waters. In *Ocean Circulation and Climate: Observing and Modelling the Global Ocean*, ed. G Siedler, J Church, J Gould, pp. 373–86. San Diego, CA: Academic
Hartmann DL, Klein Tank AMG, Rusticucci M, Alexander LV, Brönnimann S, et al. 2014. Observations: atmosphere and surface. In *Climate Change 2013: The Physical Science Basis; Contribution of Working Group I to the Fifth Assessment Report of the Intergovernmental Panel on Climate Change*, ed. TF Stocker, D Qin, G-K Plattner, M Tignor, SK Allen, et al., pp. 159–254. Cambridge, UK: Cambridge Univ. Press
Helm KP, Bindoff NL, Church JA. 2010. Changes in the global hydrological-cycle inferred from ocean salinity. *Geophys. Res. Lett.* 37:L18701
Holte JW, Talley LD. 2009. A new algorithm for finding mixed layer depths with applications to Argo data and Subantarctic Mode Water formation. *J. Atmos. Ocean. Technol.* 26:1920–39
Holte JW, Talley LD, Chereskin TK, Sloyan BM. 2013. Subantarctic Mode Water in the southeast Pacific: effect of exchange across the Subantarctic Front. *J. Geophys. Res. Oceans* 118:2052–66
Holte JW, Talley LD, Gilson J, Roemmich D. 2017. An Argo mixed layer climatology and database. *Geophys. Res. Lett.* 44:5618–26
Hosoda S, Ohira T, Sato K, Suga T. 2010. Improved description of global mixed-layer depth using Argo profiling floats. *J. Oceanogr.* 66:773–87
Hosoda S, Suga T, Shikama N, Mizuno K. 2009. Global surface layer salinity change detected by Argo and its implication for hydrological cycle intensification. *J. Oceanogr.* 65:579–86
Hou AY, Kakar RK, Neeck S, Azarbarzin AA, Kummerow CD, et al. 2014. The Global Precipitation Measurement mission. *Bull. Am. Meteorol. Soc.* 95:701–22
Huang B, Shin C-S, Kumar A, L'Heureux M, Balmaseda MA. 2021. The relative roles of decadal climate variations and changes in the ocean observing system on seasonal prediction skill of tropical Pacific SST. *Clim. Dyn.* 56:3045–63
Johnson GC, Birnbaum AN. 2017. As El Niño builds, Pacific Warm Pool expands, ocean gains more heat. *Geophys. Res. Lett.* 44:438–45
Johnson GC, Cadot C, Lyman JM, McTaggart KE, Steffen EL. 2020. Antarctic Bottom Water warming in the Brazil Basin: 1990s through 2020, from WOCE to Deep Argo. *Geophys. Res. Lett.* 47:e2020GL089191
Johnson GC, Lyman JM. 2020. Warming trends increasingly dominate global ocean. *Nat. Clim. Change* 10:757–61
Johnson GC, Lyman JM, Boyer T, Cheng L, Domingues CM, et al. 2019a. Ocean heat content. *Bull. Am. Meteorol. Soc.* 100:S74–76
Johnson GC, Lyman JM, Loeb NG. 2016. Improving estimates of Earth's energy imbalance. *Nat. Clim. Change* 6:639–40
Johnson GC, Lyman JM, Purkey SG. 2015. Informing Deep Argo array design using Argo and full-depth hydrographic section data. *J. Atmos. Ocean. Technol.* 32:2187–98
Johnson GC, Purkey SG, Zilberman NV, Roemmich D. 2019b. Deep Argo quantifies bottom water warming rates in the southwest Pacific basin. *Geophys. Res. Lett.* 46:2662–69
Johnson GC, Schmidtko S, Lyman JM. 2012. Relative contributions of temperature and salinity to seasonal mixed layer density changes and horizontal density gradients. *J. Geophys. Res. Oceans* 117:C04015

Jones DC, Holt HJ, Meijers AJS, Shuckburgh E. 2019. Unsupervised clustering of Southern Ocean Argo float temperature profiles. *J. Geophys. Res. Oceans* 124:390–402

Katsumata K. 2016. Eddies observed by Argo Floats. Part I: eddy transport in the upper 1000 dbar. *J. Phys. Oceanogr.* 46:3471–86

Kawai Y, Hosoda S, Uehara K, Suga T. 2021. Heat and salinity transport between the permanent pycnocline and the mixed layer due to the obduction process evaluated from a gridded Argo dataset. *J. Oceanogr.* 77:75–92

King BA, Firing E, Joyce TM. 2001. Shipboard observations during WOCE. In *Ocean Circulation and Climate: Observing and Modelling the Global Ocean*, ed. G Siedler, J Church, J Gould, pp. 99–122. San Diego, CA: Academic

King RR, Lea DJ, Martin MJ, Mirouze I, Heming J. 2020. The impact of Argo observations in a global weakly coupled ocean-atmosphere data assimilation and short-range prediction system. *Q. J. R. Meteorol. Soc.* 146:401–14

Kolodziejczyk N, Llovel W, Portela E. 2019. Interannual variability of upper ocean water masses as inferred from Argo array. *J. Geophys. Res. Oceans* 124:6067–85

Kumar A, Chen M, Xue Y, Behringer D. 2015. An analysis of the temporal evolution of ENSO prediction skill in the context of the equatorial Pacific Ocean observing system. *Mon. Weather Rev.* 143:3204–13

Kushnir Y, Scaife AA, Arritt R, Balsamo G, Boer G, et al. 2019. Towards operational predictions of the near-term climate. *Nat. Clim. Change* 9:94–101

Kwon YO, Riser SC. 2004. North Atlantic Subtropical Mode Water: a history of ocean-atmosphere interaction 1961–2000. *Geophys. Res. Lett.* 31:L19307

Lavender KL, Davis RE, Owens WB. 2000. Mid-depth recirculation observed in the interior Labrador and Irminger seas by direct velocity measurements. *Nature* 407:66–69

Laxenaire R, Speich S, Stegner A. 2019. Evolution of the thermohaline structure of one Agulhas ring reconstructed from satellite altimetry and Argo floats. *J. Geophys. Res. Oceans* 124:8969–9003

Laxenaire R, Speich S, Stegner A. 2020. Agulhas ring heat content and transport in the South Atlantic estimated by combining satellite altimetry and Argo profiling floats data. *J. Geophys. Res. Oceans* 125:e2019JC015511

Lea DJ, Mirouze I, Martin MJ, King RR, Hines A, et al. 2015. Assessing a new coupled data assimilation system based on the Met Office Coupled Atmosphere-Land-Ocean-Sea Ice Model. *Mon. Weather Rev.* 143:4678–94

Leuliette EW. 2015. The balancing of the sea-level budget. *Curr. Clim. Change Rep.* 1:185–91

Levitus S, Antonov J, Boyer T. 2005. Warming of the world ocean, 1955–2003. *Geophys. Res. Lett.* 32:L02604

Li G, Cheng L, Zhu J, Trenberth KE, Mann ME, Abraham JP. 2020. Increasing ocean stratification over the past half-century. *Nat. Clim. Change* 10:1116–23

Lin I-I, Chen C-H, Pun I-F, Liu WT, Wu C-C. 2009. Warm ocean anomaly, air sea fluxes, and the rapid intensification of tropical cyclone Nargis (2008). *Geophys. Res. Lett.* 36:L03817

Lozier MS, Dave AC, Palter JB, Gerber LM, Barber RT. 2011. On the relationship between stratification and primary productivity in the North Atlantic. *Geophys. Res. Lett.* 38:L18609

Majumder S, Schmid C, Halliwell G. 2016. An observations and model-based analysis of meridional transports in the South Atlantic. *J. Geophys. Res. Oceans* 121:5622–38

Meehl GA, Goddard L, Boer G, Burgman R, Branstator G, et al. 2014. Decadal climate prediction: an update from the trenches. *Bull. Am. Meteorol. Soc.* 95:243–67

Meehl GA, Goddard L, Murphy J, Stouffer RJ, Boer G, et al. 2009. Decadal prediction: Can it be skillful? *Bull. Am. Meteorol. Soc.* 90:1467–85

Mrvaljevic RK, Black PG, Centurioni LR, Chang Y-T, D'Asaro EA, et al. 2013. Observations of the cold wake of Typhoon Fanapi (2010). *Geophys. Res. Lett.* 40:316–21

Munk W. 2003. Ocean freshening, sea level rising. *Science* 300:2041–43

Nagano A, Hasegawa T, Ueki I, Ando K. 2017. El Niño–Southern Oscillation-time scale covariation of sea surface salinity and freshwater flux in the western tropical and northern subtropical Pacific. *Geophys. Res. Lett.* 44:6895–903

Oka E, Kouketsu S, Toyama K, Uehara K, Kobayashi T, et al. 2011. Formation and subduction of central mode water based on profiling float data, 2003–08. *J. Phys. Oceanogr.* 41:113–29

Oka E, Qiu B, Takatani Y, Enyo K, Sasano D, et al. 2015. Decadal variability of Subtropical Mode Water subduction and its impact on biogeochemistry. *J. Oceanogr.* 71:389–400
Oke PR, Balmaseda MA, Benkiran M, Cummings JA, Dombrowsky E, et al. 2009. Observing system evaluations using GODAE systems. *Oceanography* 22(3):144–53
Olita A, Capet A, Claret M, Mahadevan A, Poulain PM, et al. 2017. Frontal dynamics boost primary production in the summer stratified Mediterranean sea. *Ocean Dyn.* 67:767–82
Oliver ECJ, Benthuysen JA, Darmaraki S, Donat MG, Hobday AJ, et al. 2021. Marine heatwaves. *Annu. Rev. Mar. Sci.* 13:313–42
Ollitrault M, Colin de Verdière A. 2014. The ocean general circulation near 1000-m depth. *J. Phys. Oceanogr.* 44:384–409
Ollitrault M, Rannou J-P. 2013. ANDRO: an Argo-based deep displacement dataset. *J. Atmos. Ocean. Technol.* 30:759–88
Park JJ, Kwon Y-O, Price JF. 2011. Argo array observation of ocean heat content changes induced by tropical cyclones in the North Pacific. *J. Geophys. Res.* 116:C12025
Pauthenet E, Roquet F, Madec G, Sallée J-B, Nerini D. 2019. The thermohaline modes of the global ocean. *J. Phys. Oceanogr.* 49:2535–52
Piecuch CG, Quinn KJ. 2016. El Niño, La Niña, and the global sea level budget. *Ocean Sci.* 12:1165–77
Piron A, Thierry V, Mercier H, Caniaux G. 2017. Gyre-scale deep convection in the subpolar North Atlantic Ocean during winter 2014–2015. *Geophys. Res. Lett.* 44:1439–47
Portela E, Kolodziejczyk N, Maes C, Thierry V. 2020. Interior water-mass variability in the Southern Hemisphere oceans during the last decade. *J. Phys. Oceanogr.* 50:361–81
Purkey SG, Johnson GC. 2013. Antarctic Bottom Water warming and freshening: contributions to sea level rise, ocean freshwater budgets, and global heat gain. *J. Clim.* 26:6105–22
Qu T, Gao S, Fukumori I, Fine RA, Lindstrom EJ. 2008. Subduction of South Pacific waters. *Geophys. Res. Lett.* 35:L02610
Qu T, Yu J-Y. 2014. ENSO indices from sea surface salinity observed by Aquarius and Argo. *J. Oceanogr.* 70:367–75
Qu T, Zhang L, Schneider N. 2016. North Atlantic subtropical underwater and its year-to-year variability in annual subduction rate during the Argo period. *J. Phys. Oceanogr.* 46:1901–16
Riser SC, Freeland HJ, Roemmich D, Wijffels S, Troisi A, et al. 2016. Fifteen years of ocean observations with the global Argo array. *Nat. Clim. Change* 6:145–53
Roach CJ, Balwada D, Speer K. 2016. Horizontal mixing in the Southern Ocean from Argo float trajectories. *J. Geophys. Res. Oceans* 121:5570–86
Roach CJ, Balwada D, Speer K. 2018. Global observations of horizontal mixing from Argo float and surface drifter trajectories. *J. Geophys. Res. Oceans* 123:4560–75
Roberts MJ, Jackson LC, Roberts CD, Meccia V, Docquier D, et al. 2020. Sensitivity of the Atlantic Meridional Overturning Circulation to model resolution in CMIP6 HighResMIP simulations and implications for future changes. *J. Adv. Model. Earth Syst.* 12:e2019MS002014
Robson JI, Aksenov Y, Bracegirdle TJ, Dimdore-Miles O, Griffiths PT, et al. 2020. The evaluation of the North Atlantic Climate System in UKESM1 historical simulations for CMIP6. *J. Adv. Model. Earth Syst.* 12:e2020MS002126
Robson JI, Sutton RT, Smith DM. 2012. Initialized decadal predictions of the rapid warming of the North Atlantic Ocean in the mid 1990s. *Geophys. Res. Lett.* 39:L19713
Roemmich D, Gilson J. 2009. The 2004–2008 mean and annual cycle of temperature, salinity, and steric height in the global ocean from the Argo Program. *Prog. Oceanogr.* 82:81–100
Roemmich D, Gilson J. 2011. The global ocean imprint of ENSO. *Geophys. Res. Lett.* 38:L13606
Roemmich D, Gilson J, Sutton P, Zilberman N. 2016. Multidecadal change of the South Pacific Gyre circulation. *J. Phys. Oceanogr.* 46:1871–83
Roemmich D, Gould WJ, Gilson J. 2012. 135 years of global ocean warming between the *Challenger* expedition and the Argo Programme. *Nat. Clim. Change* 2:425–28
Roullet G, Capet X, Maze G. 2014. Global interior eddy available potential energy diagnosed from Argo floats. *Geophys. Res. Lett.* 41:1651–56

Sallee JB, Speer K, Rintoul S, Wijffels S. 2010. Southern Ocean thermocline ventilation. *J. Phys. Oceanogr.* 40:509–29

Sasaki YN, Schneider N, Maximenko N, Lebedev K. 2010. Observational evidence for propagation of decadal spiciness anomalies in the North Pacific. *Geophys. Res. Lett.* 37:L07708

Scannell HA, Johnson GC, Thompson L, Lyman JM, Riser SC. 2020. Subsurface evolution and persistence of marine heatwaves in the northeast Pacific. *Geophys. Res. Lett.* 47:e2020GL090548

Schanze JJ, Schmitt RW, Yu LL. 2010. The global oceanic freshwater cycle: a state-of-the-art quantification. *J. Mar. Res.* 68:569–95

Schmidtko S, Johnson GC, Lyman JM. 2013. MIMOC: a global monthly isopycnal upper-ocean climatology with mixed layers. *J. Geophys. Res. Oceans* 118:1658–72

Stockdale T, Alonso-Balmaseda M, Johnson S, Ferranti L, Molteni F, et al. 2018. *SEAS5 and the future evolution of the long-range forecast system*. Tech. Memo. 835, Eur. Cent. Medium-Range Weather Forecasts, Berkshire, UK. **https://doi.org/10.21957/z3e92di7y**

Stommel H. 1957. Abyssal circulation of the ocean. *Nature* 180:733–34

Storto A, Alvera-Azcárate A, Balmaseda MA, Barth A, Chevallier M, et al. 2019. Ocean reanalyses: recent advances and unsolved challenges. *Front. Mar. Sci.* 6:418

Sun B, Liu C, Wang F. 2019. Global meridional eddy heat transport inferred from Argo and altimetry observations. *Sci. Rep.* 9:1345

Thompson PR, Widlansky MJ, Leuliette E, Sweet W, Chambers DP, et al. 2020. Sea level variability and change. *Bull. Am. Meteorol. Soc.* 101:S153–56

Tizard TH, Moseley HN, Buchanan JY, Murray J. 1965 (1885). Chapter III. In *The Voyage of H.M.S. Challenger: Narrative of the Cruise of H.M.S. Challenger with a General Account of the Scientific Results of the Expedition*, ed. C Wyville Thompson, J Murray, Vol. I, First Part, pp. 83–120. New York: Johnson Repr. Corp. **https://archimer.ifremer.fr/doc/00000/4751**

Toyama K, Iwasaki A, Suga T. 2015. Interannual variation of annual subduction rate in the North Pacific estimated from a gridded Argo product. *J. Phys. Oceanogr.* 45:2276–93

Trenberth KE, Fasullo JT. 2017. Atlantic meridional heat transports computed from balancing Earth's energy locally. *Geophys. Res. Lett.* 44:1919–27

Trossman DS, Thompson L, Kelly KA, Kwon YO. 2009. Estimates of North Atlantic ventilation and mode water formation for winters 2002–06. *J. Phys. Oceanogr.* 39:2600–17

Vellinga M, Copsey D, Graham T, Milton S, Johns T. 2020. Evaluating benefits of two-way ocean–atmosphere coupling for global NWP forecasts. *Weather Forecast.* 35:2127–44

Voldoire A, Saint-Martin D, Sénési S, Decharme B, Alias A, et al. 2019. Evaluation of CMIP6 DECK experiments with CNRM-CM6-1. *J. Adv. Model. Earth Syst.* 11:2177–213

von Schuckmann K, Cheng LJ, Palmer MD, Hansen J, Tassone C, et al. 2020. Heat stored in the Earth system: Where does the energy go? *Earth Syst. Sci. Data* 12:2013–41

Wang X, Bhatt V, Sun Y-J. 2015. Seasonal and inter-annual variability of western subtropical mode water in the South Pacific Ocean. *Ocean Dyn.* 65:143–54

Warren B. 1981. Deep circulation of the world ocean. In *Evolution of Physical Oceanography: Scientific Surveys in Honor of Henry Stommel*, ed. BA Warren, C Wunsch, pp. 6–41. Cambridge, MA: MIT Press

Whalen CB, MacKinnon JA, Talley LD, Waterhouse AF. 2015. Estimating the mean diapycnal mixing using a finescale strain parameterization. *J. Phys. Oceanogr.* 45:1174–88

Wijffels S, Roemmich D, Monselesan D, Church J, Gilson J. 2016. Ocean temperatures chronicle the ongoing warming of Earth. *Nat. Clim. Change* 6:116–18

Willis JK. 2010. Can in situ floats and satellite altimeters detect long-term changes in Atlantic Ocean overturning? *Geophys. Res. Lett.* 37:L06602

Wong APS, Wijffels SE, Riser SC, Pouliquen S, Hosoda S, et al. 2020. Argo data 1999–2019: two million temperature-salinity profiles and subsurface velocity observations from a global array of profiling floats. *Front. Mar. Sci.* 7:700

Woolnough SJ, Vitart F, Balmaseda MA. 2007. The role of the ocean in the Madden–Julian Oscillation: implications for MJO prediction. *Q. J. R. Meteorol. Soc.* 133:117–28

Yang J, Riser SC, Nystuen JA, Asher WE, Jessup AT. 2015. Regional rainfall measurements using the Passive Aquatic Listener during the SPURS field campaign. *Oceanography* 28(1):124–33

Yeager S, Karspeck A, Danabasoglu G, Tribbia J, Teng HY. 2012. A decadal prediction case study: late twentieth-century North Atlantic Ocean heat content. *J. Clim.* 25:5173–89

Zanowski H, Johnson GC, Lyman JM. 2019. Equatorial Pacific 1,000-dbar velocity and isotherm displacements from Argo data: beyond the mean and seasonal cycle. *J. Geophys. Res. Oceans* 124:7873–82

Zhang S, Liu Z, Zhang X, Wu X, Han G, et al. 2020. Coupled data assimilation and parameter estimation in coupled ocean-atmosphere models: a review. *Clim. Dyn.* 54:5127–44

Zhang Z, Wang W, Qiu B. 2014. Oceanic mass transport by mesoscale eddies. *Science* 345:322–24

Zhang Z, Zhang Y, Wang W, Huang RX. 2013. Universal structure of mesoscale eddies in the ocean. *Geophys. Res. Lett.* 40:3677–81

Zhao M, Hendon HH, Alves O, Liu G, Wang G. 2016. Weakened eastern Pacific El Niño predictability in the early twenty-first century. *J. Clim.* 29:6805–22

Zhu Y, Zhang R, Sun J. 2020. North Pacific upper-ocean cold temperature biases in CMIP6 simulations and the role of regional vertical mixing. *J. Clim.* 33:7523–38

Zilberman NV, Roemmich DH, Gille ST. 2014. Meridional volume transport in the South Pacific: mean and SAM-related variability. *J. Geophys. Res. Oceans* 119:2658–78

Zuo H, Balmaseda MA, Tietsche S, Mogensen K, Mayer M. 2019. The ECMWF operational ensemble reanalysis–analysis system for ocean and sea ice: a description of the system and assessment. *Ocean Sci.* 15:779–808